

Theoretical Study on the Regioselectivity of Electrophilic Aromatic Substitution Reactions of Azulene

Nader Zabarjad Shiraz,* Elaheh Sadat Sharifzadeh and Neda Koosha

Department of Chemistry, Islamic Azad University, Central Tehran Branch, 146786831, Tehran, IRAN

* Corresponding author: E-mail: zabarjad_sh@yahoo.com

Received: 23-04-2012

Abstract

In this study electrophilic affinities were calculated at all reactive positions of azulene in electrophilic aromatic substitutions. Structures of cationic intermediates and products were optimized at HF/6-31+G* and B3LYP/6-31+G** levels of theory, and single point calculations were carried out at MP2/6-31+G**//B3LYP/6-31+G** for total energy. NICS calculations, activation energies and relative stabilities (ΔE) were used to predict the most reactive site in azulene. Results indicated that position 1 is the most reactive site for electrophilic aromatic reactions in terms of kinetic considerations, while the isomers with substituents at position 2 are predominantly thermodynamic products.

Keywords: Ab initio calculations; Azulene; Electrophilic Aromatic Reaction; NICS

1. Introduction

Azulene (AZ), cross conjugated aromatic system composed of 5- and 7-member rings, is resonance stabilized bicyclic 10- π electron system and has hybrid structure of formal combination of two charged sextets of cyclopentadienyl anion (**1a**) and the tropylium cation (**1b**) (Scheme 1).¹ It was synthesized in 1937 for the first time.² In ancient Egypt, azulene derivatives were used for dyeing cotton. Azulene was generated from several kinds of plants through distillation, extraction, and other chemical treatment.³



Scheme 1. Possible mesomeric structures of azulene.

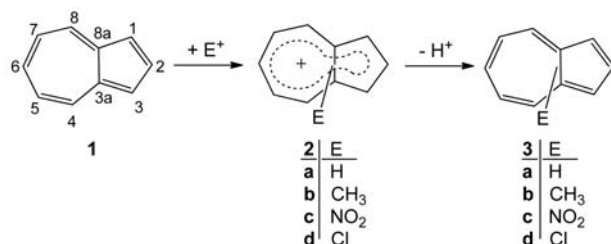
Study of azulene has become one of the popular topics in organic, medical, and theoretical chemistry as well as in dye industry. Several theoretical studies of azulene have been published using semiempirical, ab initio, and DFT calculations.⁴⁻⁷ Experimentally, several attempts have been made to determine the molecular structure of azulene based on the X-ray analysis.⁸⁻¹¹ Neither theoretic

cal calculations nor experimental investigations have completely resolved the geometry of the ground state structure of azulene, i.e., ab initio calculations had predicted the localized structure (C_s symmetry), despite the later DFT calculation predicted a C_{2v} symmetry which corresponds to delocalized structure.⁷

In accordance with such considerations, electrophilic reagent reacts with azulene in a way reminiscent of their behavior toward fullerenes and the cyclopentadienyl anion. Therefore, the electrophilic attack takes place at 5-member ring and is concomitant with the formation of tropylium cation. Electrophilic substitution of azulene including halogenations, nitration, and Friedel-Crafts acetylation resulted in mainly 1-substituted azulene derivatives.^{12,13} In some cases comprising Vilsmeier formylation reaction proceeded regioselectively at position 2.¹⁴

Although calculations, spectroscopic data, as well as other physical properties provide more accurate geometric structure for azulene and its derivatives, there were infrequent theoretical studies concerning the regioselectivity of AZ in electrophilic aromatic reactions (EARs). Calculations at 6-31+G* level were in agreement with experiment for proton affinities of benzoid hydrocarbons.¹⁵ Given the rising interest in AZ and its properties in electrophilic aromatic substitutions, along with very scarce informations¹⁶ concerning azulene reactions, was the impetus to predict the regioselectivity of EARs at all reactive positions of AZ in the present study.

The structures of azulene (**1**), its carbocation intermediates (**2**) and products (**3**) (Scheme 2) were fully optimized without constrain in EARs. According to the geometry analysis, AZ has 5 reactive sites in EARs (position 1, 2, 4, 5 and 6; Scheme 2), and for each reaction path transition states and intermediates were investigated.



Scheme 2. Electrophilic aromatic substitution reactions of azulene (E at position 1, 2, 4, 5 and 6).

2. Calculations

Calculations were performed at HF/6-31+G* and B3LYP/6-31+G** levels of theory for geometry optimization and at MP2/6-31+G**/B3LYP/6-31+G** level for a single point total energy calculations, using procedures

implemented in the Gaussian 98 package.¹⁷ Vibrational frequencies were calculated for all geometries, which were confirmed to have zero imaginary frequency. The frequencies were scaled by a factor of 0.9135 for HF method and used for computation of the zero-point vibrational energies.^{18,19} Theoretical absolute NMR shielding was calculated using the Gauge Invariant Atomic Orbitals (GIAO) method at the same computational level. For the Negative Nucleus-Independent Chemical Shift (NICS) values, the sign convention for isotropic values used by other authors, that is, negative for aromatic compounds and positive for anti aromatic ones, was followed.²⁰

3. Results and Discussion

The results of ab initio calculations, total electronic energies (HF, Hartree) along with the values of relative energies (ΔE , kcal/mol) at HF/6-31+G*, B3LYP/6-31+G**, and MP2/6-31+G**/B3LYP/6-31+G** levels of theory have been listed in Tables 1-6 for AZ (**1**), 20 intermediates (**2**) and 15 products (**3**), resulted from EARs at 5 reactive positions indicated by the numbers (see Scheme 2).

Table 1. Calculated HF (Hartree), ZPE (Hartree/particle) and ΔE (kcal/mol) of intermediates (**2**) at HF/6-31+G* level.

Comp.	Energy	Position				
		1	2	4	5	6
2a	HF	-383.6834391	-383.6428850	-383.6176993	-383.6467142	-383.6132528
	ZPE	0.170047	0.168232	0.168436	0.16909	0.167365
	ΔE	0.00	24.31	40.24	22.44	42.36
2b	HF _a	-422.719848	-422.6796178	-422.6518598	-422.6823858	-422.6486909
	ZPE	0.200315	0.198579	0.198636	0.199458	0.198035
	ΔE	0.00	24.16	41.61	22.97	43.22
2c	HF	-587.1343711	-587.0907031	-587.0667686	-587.095434	-587.0600234
	ZPE	0.1742252	0.172574	0.173714	0.173299	0.171813
	ΔE	0.00	26.37	42.10	23.85	45.14
2d	HF	-842.5647141	-842.5268568	-842.5023369	-842.5322339	-842.4966805
	ZPE	0.160901	0.159107	0.158752	0.159904	0.158513
	ΔE	0.00	22.63	37.79	19.76	41.19

Table 2. Calculated HF (Hartree), ZPE (Hartree/particle) and ΔE (kcal/mol) of products (**3**) at HF/6-31+G* level.

Comp.	Energy	Position				
		1	2	4	5	6
3b	HF	-422.3317012	-422.3353154	-422.3297645	-422.3301118	-422.3320490
	ZPE	0.185405	0.185476	0.185609	0.185703	0.185628
	ΔE	2.35	0.00	3.57	3.41	2.14
3c	HF	-586.7782299	-586.7746864	-586.7605956	-586.7713880	-586.7667625
	ZPE	0.157653	0.159504	0.157708	0.158525	0.159858
	ΔE	0.00	3.39	11.10	4.84	8.58
3d	HF	-842.1952289	-842.1966114	-842.1911456	-842.1917527	-842.1926081
	ZPE	0.14643	0.145972	0.145886	0.146021	0.145931
	ΔE	1.16	0.00	3.38	3.08	2.49

Table 3. Calculated HF (Hartree) and ΔE (kcal/mol) of intermediates **2** at B3LYP/6-31+G** level.

Comp.	Energy	Position				
		1	2	4	5	6
2a	HF	-386.2359531	-386.1995863	-386.17089	-386.2015276	-386.1752751
	ΔE	0.00	22.82	40.83	21.60	38.08
2b	HF	-425.5550203	-425.518948	-425.4879525	-425.5197785	-425.4925736
	ΔE	0.00	22.64	42.09	22.11	39.19
2c	HF	-590.7182992	-590.6782652	-590.63915	-590.6824491	-590.6517782
	ΔE	0.00	25.12	49.67	22.50	41.74
2d	HF	-845.8157374	-845.7751776	-845.7473754	-845.780647	-845.7487789
	ΔE	0.00	25.45	42.90	22.02	42.02

Table 4. Calculated HF (Hartree) and ΔE (kcal/mol) of products **3** at B3LYP/6-31+G** level.

Comp.	Energy	Position				
		1	2	4	5	6
3b	HF	-425.1864041	-425.1888785	-425.1838319	-425.1840453	-425.1855700
	ΔE	1.55	0.00	3.17	3.03	2.08
3c	HF	-590.3802695	-590.3761348	-590.3648470	-590.3757659	-590.3715843
	ΔE	0.00	2.59	9.68	2.83	5.45
3d	HF	-845.4598051	-845.4620705	-845.4588086	-845.4579270	-845.4594513
	ΔE	1.42	0.00	2.05	2.60	1.64

Table 5. Calculated MP2 (Hartree) and ΔE (kcal/mol) energies of intermediates **2** at MP2/6-31+G**//B3LYP/6-31+G** level.

Comp.	Energy	Position				
		1	2	4	5	6
2a	MP2	-385.0083651	-384.961346	-384.9298033	-384.9636918	-384.932948
	ΔE	0.00	29.50	49.30	28.03	47.32
2b	MP2	-424.1970878	-424.1493238	-424.1180878	-424.15159	-424.1195975
	ΔE	0.00	29.97	49.57	28.55	48.63
2c	MP2	-589.0026664	-588.9490249	-588.9147798	-588.9546768	-588.9184965
	ΔE	0.00	33.66	55.15	30.11	52.82
2d	MP2	-844.0218046	-843.9694257	-843.9429	-843.9754596	-843.9392346
	ΔE	0.00	32.87	49.51	29.08	51.81

Table 6. Calculated MP2 (Hartree) and ΔE (kcal/mol) energies of products **3** at MP2/6-31+G**//B3LYP/6-31+G** level.

Comp.	Energy	Position				
		1	2	4	5	6
3b	MP2	-423.83158	-423.8331314	-423.8295206	-423.8295546	-423.830318
	ΔE	0.97	0.00	2.27	2.24	1.77
3c	MP2	-588.6536739	-588.658728	-588.6375943	-588.6572233	-588.657286
	ΔE	3.17	0.00	13.26	0.94	0.90
3d	MP2	-843.6698331	-843.671167	-843.6704244	-843.6676137	-843.6693343
	ΔE	0.84	0.00	0.47	2.23	1.15

Considering the optimized structures, intermediates **2** were conjugated carbocations, however, no proper resonance was observed; carbon-carbon bonds are alternate single and double bonds, although slight partial resonance shortened single C–C bonds to 1.43 Å (see Figure 1).

The existence of tropylium-like cation resulting from the substitution at position-1, made the most stable intermediate **2**. The bond lengths of 7-member ring were more similar than that of 5-member ring (Figure 1).

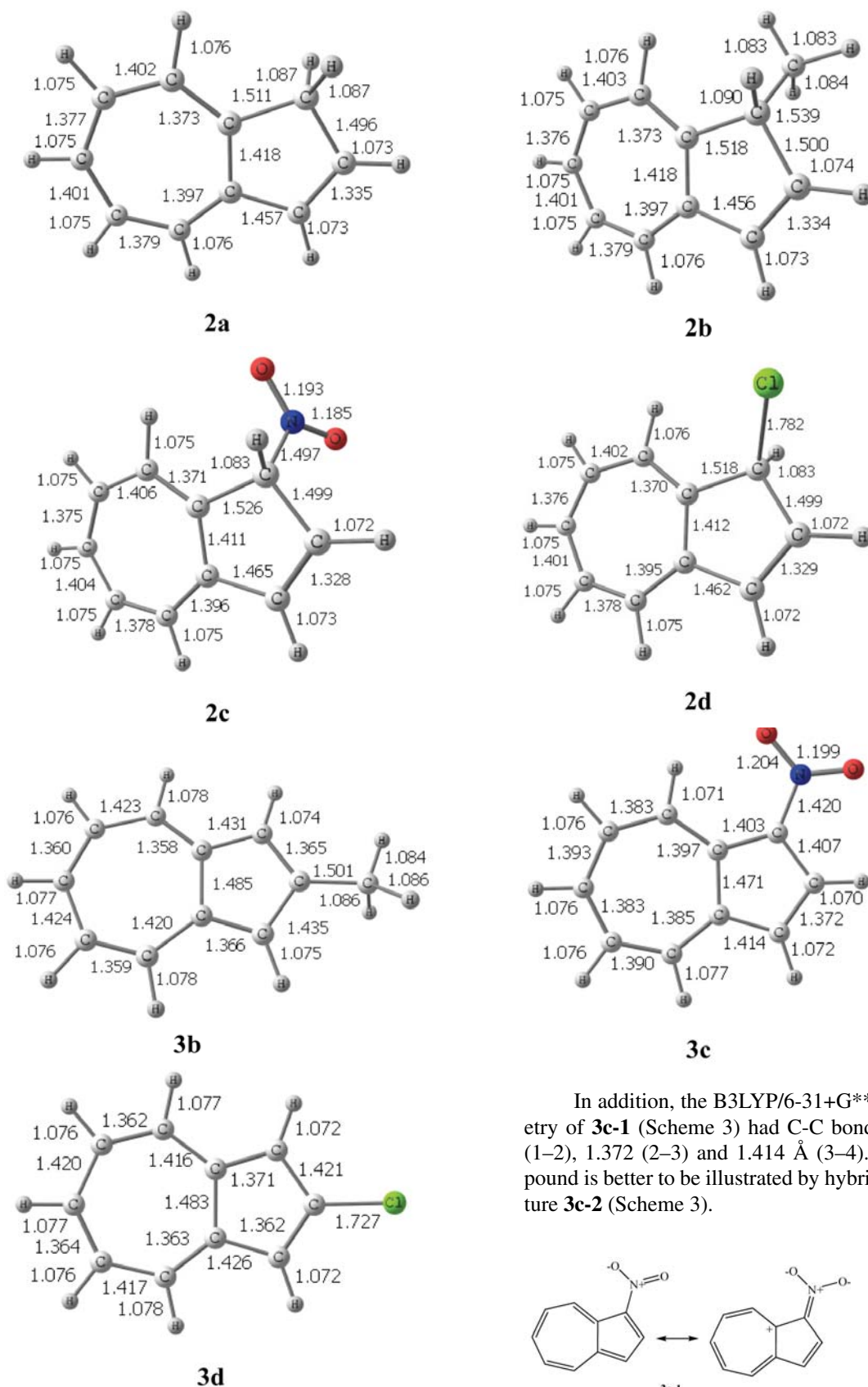
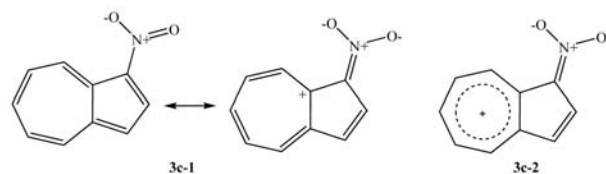
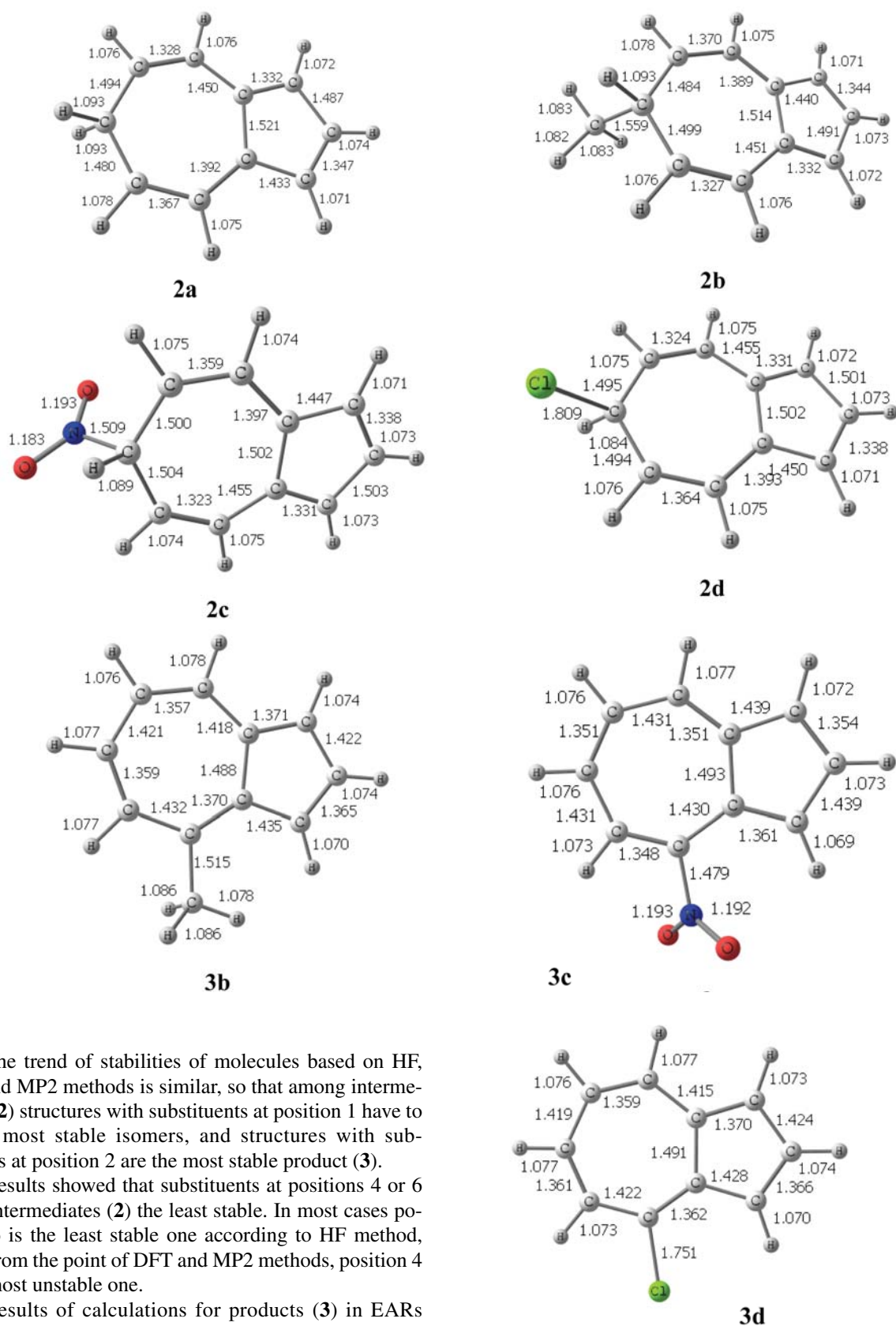


Figure 1. The most stable isomers of intermediates (**2**) and products (**3**) optimized at the B3LYP/6-31+G** level of theory.

In addition, the B3LYP/6-31+G** optimized geometry of **3c-1** (Scheme 3) had C-C bond lengths of 1.407 (1–2), 1.372 (2–3) and 1.414 Å (3–4). Clearly the compound is better to be illustrated by hybrid resonance structure **3c-2** (Scheme 3).



Scheme 3. Mesomeric structures of nitroazulene (**3c**)



The trend of stabilities of molecules based on HF, DFT and MP2 methods is similar, so that among intermediates (**2**) structures with substituents at position 1 have to be the most stable isomers, and structures with substituents at position 2 are the most stable product (**3**).

Results showed that substituents at positions 4 or 6 made intermediates (**2**) the least stable. In most cases position 6 is the least stable one according to HF method, while from the point of DFT and MP2 methods, position 4 is the most unstable one.

Results of calculations for products (**3**) in EARs comparing CH_3 , NO_2 , and Cl as electrophiles revealed that except for NO_2 group, which deviated from the trend of stability, products having substituents at position 2 in

Figure 2. The least stable isomers of intermediates (**2**) and products (**3**) optimized at the B3LYP/6-31+G** level of theory.

azulene are the most stable isomer. In structure **3c**, for example, position 1 is the most stable one. Structure **3c-2** (Scheme 3) possessing some stable tropylium cation character could explain the excessive stability of this product. Comparison of relative energies showed that products possessing substituents at position-4 are thermodynamically the least stable. The stabilities of structures with substituents at other positions varied with different substituents. The optimized structural parameters of the most and the least stable products (**3**) are summarized in Figures 1 and 2.

According to all employed methods, relative energies (ΔE) between the most and the least stable isomers of products (**3**) were less than 13.26 kcal/mol. However, these value for parent intermediates (**2**) increased to 55.15 kcal/mol (Tables 1-6). This suggested that substituents have greater influence on the stability of intermediates (**2**) rather than on the stability of products (**3**). Therefore, in terms of kinetic considerations, substituents

could play more prominent role in the control of regioselectivity of EARs.

As can be seen from Tables 1–6, positions 1 and 2 are the dominant competitors in regioselectivity of azulene in EARs. To have a clearer picture about the regioselectivity of EARs, chlorination of azulene was simulated as an example. Hence, the structures of reagents (**F**), transition states (**G**, **I**, **K** and **M**), intermediates (**H** and **L**), and products (**J** and **N**) were optimized at B3LYP/6-31+G** level of theory and the relative energies are summarized in Table 7 and illustrated in Figure 3.

The first step of each reaction path is the rate determining step in which is reagent converted to corresponding intermediate. According to Figure 3, activation energy of path-2 ($E_{a21} = 177.8$ kcal/mol) is greater than that of path-1 ($E_{a11} = 149.0$ kcal/mol). Therefore, the reactions which took place at position-1 are under kinetic control. In terms of relative stabilities of products, path-2 suggested thermodynamic control, although the difference be-

Table 7. Calculated HF (Hartree) and ΔE (kcal/mol) of involved reagents (**F**), transition states (**G**, **I**, **K** and **M**), intermediates (**H** and **L**), and products (**J** and **N**) at B3LYP/6-31+G** level of theory.

Comp.	F	G	H	I	J
Path 1	HF	-1305.981041	-1306.090463	-1305.915518	-1306.263011
	ΔE	149.0	80.3	190.1	-27.9
Comp.	F	K	L	M	N
Path 2	HF	-1305.935105	-1306.049904	-1305.901196	-1306.265277
	ΔE	177.8	105.8	199.1	-29.4

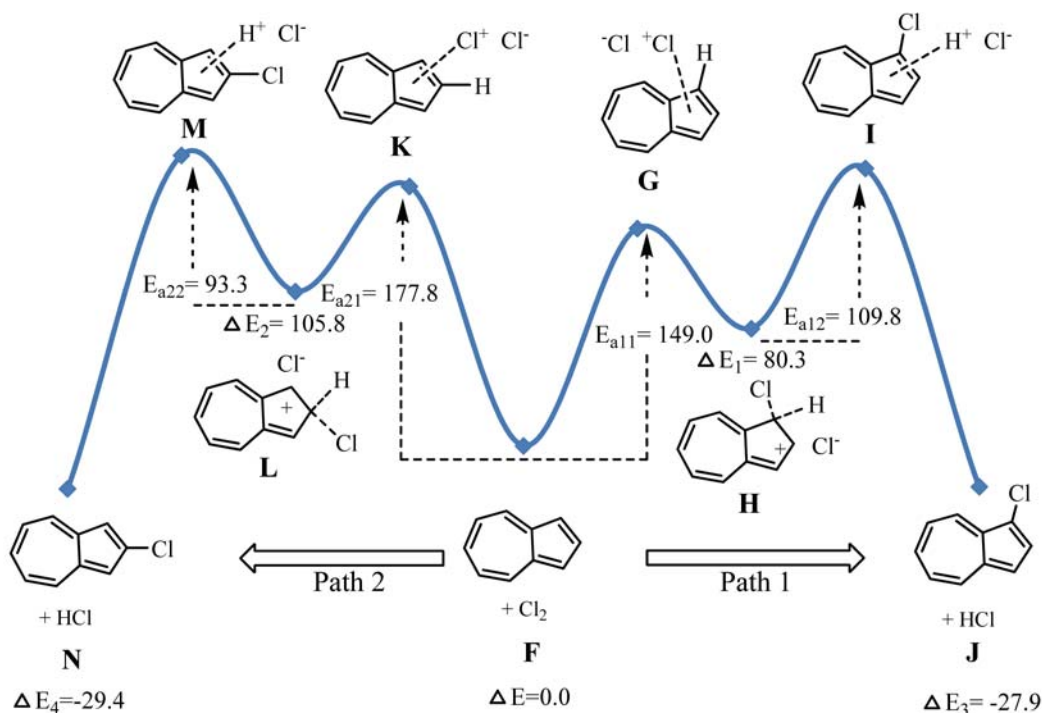


Figure 3. Energy diagram (in kcal/mol) for chlorination of azulene at positions 1 and 2

Table 8. Calculated NICS(0) values of 5- and 7-member rings of azulene and its derivatives (**3**) (Δ NICS values relate to parent product **3** in parentheses)

E	Position	Intermediate 2				Product 3					
		1	2	4	5	6	1	2	4	5	6
a	Ring (7)	-6.609 (-1.68)	8.354 (13.28)	-	-	-	-4.925	-	-	-	-
	Ring (5)	-	-	10.487 (27.23)	-3.996 (12.75)	14.053 (30.80)	-16.742	-	-	-	-
b	Ring (7)	-6.557 (-3.23)	8.186 (12.46)	-	-	-	-3.329	-4.777	-4.659	-4.423	-4.290
	Ring (5)	-	-	12.122 (28.17)	-3.935 (11.13)	15.159 (30.77)	-15.604	-15.413	-16.052	-15.064	-15.606
c	Ring (7)	-6.185 (1.71)	9.596 (13.79)	-	-	-	-7.890	-4.198	-4.777	-5.330	-4.893
	Ring (5)	-	-	14.984 (29.66)	-0.202 (17.43)	22.027 (36.02)	-17.337	-19.663	-14.674	-17.631	-13.995
d	Ring (7)	-6.546 (-2.07)	9.538 (14.17)	-	-	-	-4.481	-5.433	-5.775	-5.112	-5.065
	Ring (5)	-	-	3.427 (19.45)	-0.207 (15.31)	21.067 (36.99)	-17.227	-17.879	-16.021	-15.517	-15.919

tween relative stabilities of products is almost negligible (1.5 kcal/mol).

In order to complement the results, NICS calculations were also performed using GIAO approach at HF/6-31+G* level of theory. NICS(0) values were calculated in the center of 5- and 7-member rings (Table 8). Δ NICS values related to parent products **3** (in parentheses) are also shown in Table 8. According to Schleyer's convention,²¹ aromatic compounds have negative NICS values and antiaromatic compounds positive ones. If we take into account that the NICS(0) of azulene rings are negative, then, both rings of **3** are typically aromatic.

Comparison of NICS values of 5- and 7-member rings indicated that 5-member ring in azulene is more aromatic than 7-member ring, and that substituents have only slight effect on the aromaticity of azulene derivatives. Among studied electrophiles, the NO₂ group possesses the most pronounced effect among substituents on the NICS calculations for different positions in azulene. This may be due to the π -electron resonance of NO₂ group which could be effective in the anisotropic ring current (Scheme 3). Comparison of results of NICS calculations on intermediates **2** indicated that substitution at some positions changed aromaticity of azulene to antiaromaticity.

4. Conclusions

Ab initio calculations provided an insight on the geometries of electrophilic aromatic substitution reactions in azulene from both structural and energetic point of view. Furthermore, we have systematically evaluated the performance of NICS analysis in estimating the aromaticity in a series of skeletally mono-substituted azulenes.

Like other electrophilic substitution reactions of aromatic compounds,²² for the regioselectivity of reactions in azulene is predicted to be under kinetic control. In terms of kinetic considerations is position-1 of azulene the most reactive site in all isomers studied, while the isomers possessing substituents at position-2 are predominantly thermodynamic products. Theoretical simulation of the chlorination of azulene predicted the reaction to take place at position-1 which is in compliance with experimental findings.^{12,13} It would be insightful to have direct structural data for all azulene products for comparison with the results of ab initio calculations. In conclusion, calculations at B3LYP/6-31+G** level of theory could provide acceptable predictions of EARs for organic chemists to design synthesis of substituted azulenes.

5. References

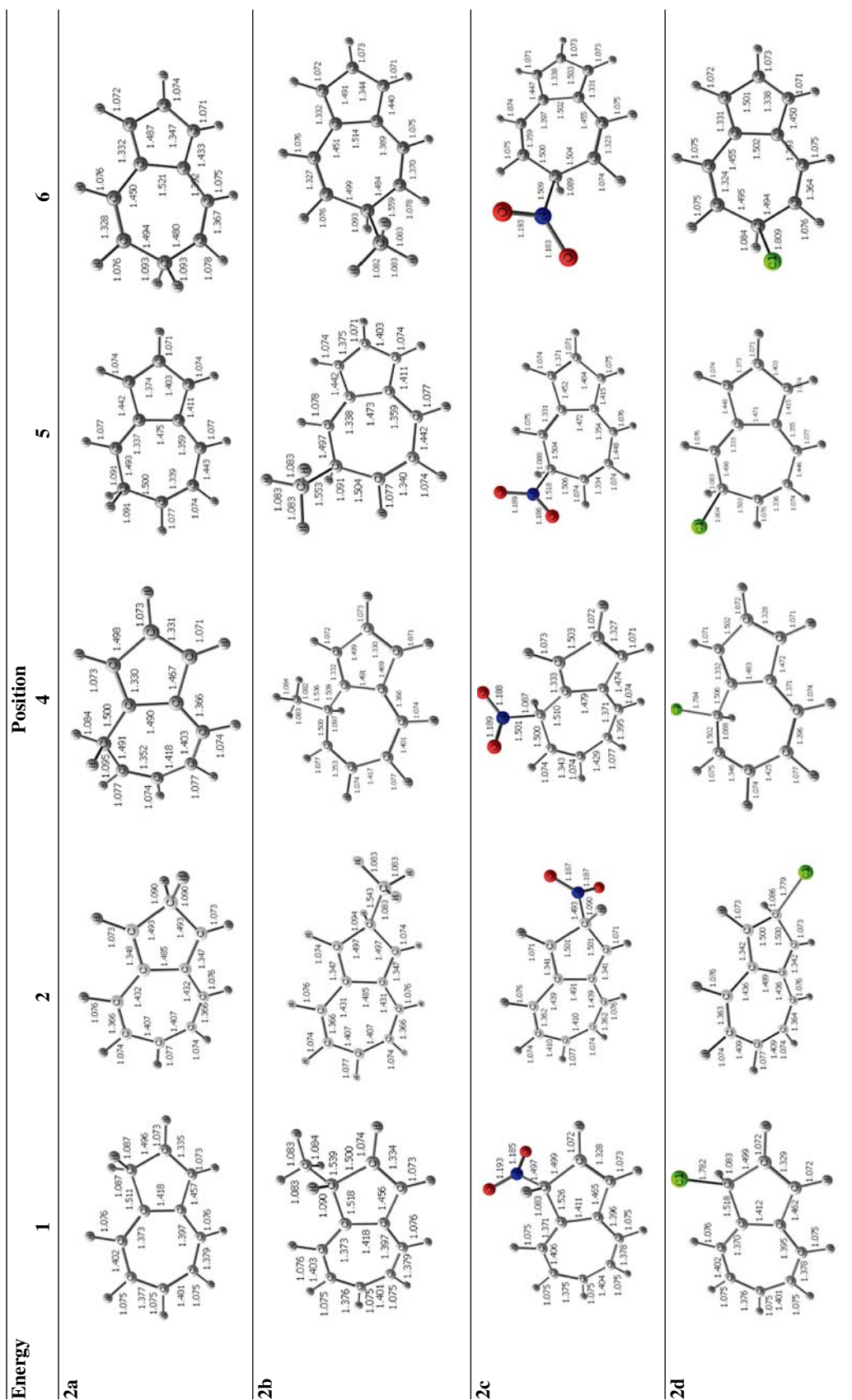
1. A. G. Anderson Jr., J. A. Nelson, *J. Am. Chem. Soc.* **1950**, *72*, 3824–3825.
2. P. A. Plattner, A. S. Pfau, *Helv. Chim. Acta* **1937**, *20*, 224–232.
3. B.-C. Wang, Y.-S. Lin, J.-C. Chang, P.-Y. Wang, *Can. J. Chem.* **2000**, *78*, 224–232.
4. R. C. Haddon, K. Raghavachari, *J. Am. Chem. Soc.* **1982**, *104*, 3516–3518.
5. R. C. Haddon, K. Raghavachari, *J. Chem. Phys.* **1983**, *79*, 1093–1094.
6. S. Grimme, *Chem. Phys. Lett.* **1993**, *201*, 67–74.
7. P. M. Kozłowski, G. Rauhut, P. Pulay, *J. Chem. Phys.* **1995**, *103*, 5650–5661.
8. J. M. Robertson, H. M. M. Shearer, G. A. Sirn, D. G. Watson, *Acta Crystallogr.* **1962**, *15*, 1–8.

9. G. S. Pawley, *Acta. Crystallogr.* **1965**, *18*, 560–561.
10. A. W. Hanson, *Acta. Crystallogr.* **1965**, *19*, 19–26.
11. K. Hafner, A. Stephan, C. Bernhard, *Liebigs Ann. Chem.* **1961**, *650*, 42–62.
12. A. G. Anderson Jr., J. A. Nelson, J. J. Tazuma, *J. Am. Chem. Soc.* **1953**, *75*, 4980–4989.
13. E. Grovenstein, F. C. Schmalstieg, *J. Am. Chem. Soc.*, **1967**, *89*, 5084–5085.
14. K. Hafner, J. Schneider, *Liebigs Ann. Chem.* **1959**, *624*, 37–47.
15. D. Z. Wang, A. Streitwieser, *Theor. Chem. Acc.* **1999**, *102*, 78–86.
16. T. Okazaki, K. K. Laali, *Org. Biomol. Chem.* **2003**, *1*, 3078–3093.
17. M. J. Frisch, G. W. Trucks, H. B. Schlegel, G. E. Scuseria, M. A. Robb, J. R. Cheeseman, V. G. Zakrzewski, J. A. Montgomery, R. E. Stratmann, J. C. Burant, S. Dapprich, J. M. Millam, A. D. Daniels, K. N. Kudin, M. C. Strain, O. Farkas, J. Tomasi, V. Barone, M. Cossi, R. Cammi, B. Mennucci, C. Pomelli, C. Adamo, S. Clifford, J. Ochterski, G. A. Petersson, P. Y. Ayala, Q. Cui, K. Morokuma, D. K. Malick, A. D. Rabuck, K. Raghavachari, J. B. Foresman, J. Cioslowski, J. V. Ortiz, B. B. Stefanov, G. Liu, A. Liashenko, P. Piskorz, I. Komaromi, R. Gomperts, R. L. Martin, D. J. Fox, T. Keith, M. A. Al-Laham, C. Y. Peng, A. Nanayakkara, C. Gonzalez, M. Challacombe, P. M. W. Gill, B. Johnson, W. Chen, M. W. Wong, J. L. Andres, C. Gonzalez, M. Head-Gordon, E. S. Replogle, J. A. Pople, Gaussian, Inc., Pittsburgh, PA, 1998.
18. R. S. Grev, C. L. Janssen, H. F. Schaefer, *J. Chem. Phys.* **1991**, *95*, 5128–5132.
19. F. Jensen, *Introduction to Computational Chemistry*; Wiley, New York, 1999.
20. S. Noorizadeh, M. Dardab, *Chem. Phys. Lett.* **2010**, *493*, 376–380.
21. W. Hehre, L. Radom, P. v. R. Schleyer, J. A. Pople, *Ab initio Molecular Orbital Theory*; Wiley, New York, 1986.
22. D. A. McCaulay, A. P. Lien, *J. Am. Chem. Soc.* **1952**, *74*, 6246–6250.

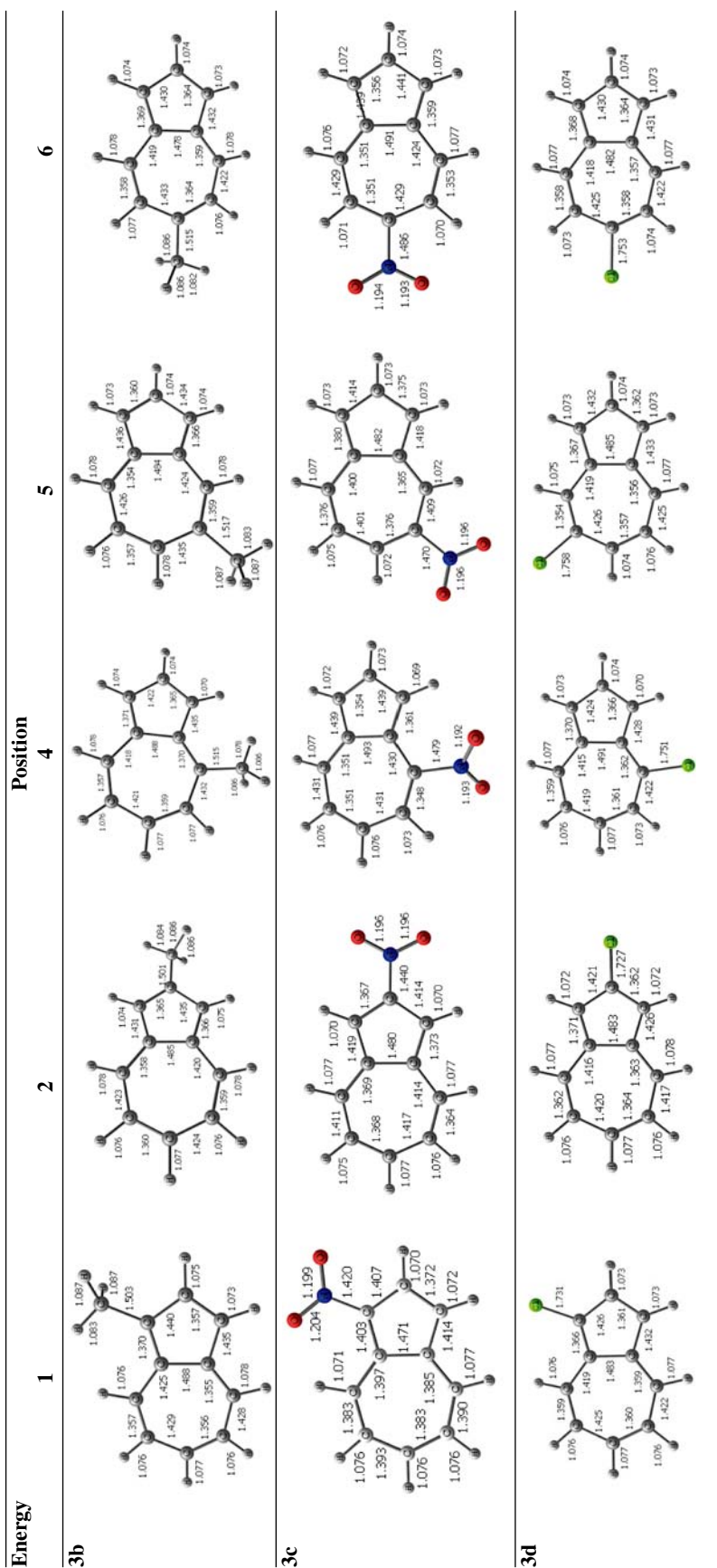
Povzetek

Prispevek podaja rezultate teoretičnih izračunov elektrofilne afinitete vseh reaktivnih mest v azulenu pri reakcijah elektrofilne aromatske substitucije. Strukture kationskih intermediatov in produktov so bile optimizirane z HF/6-31+G* in B3LYP/6-31+G** izračuni, energije optimiziranih struktur pa so bile izračunane na MP2/6-31+G**//B3LYP/6-31+G** nivoju (*single point calculations*). Najbolj reaktivna mesta v azulenu so bila določena s pomočjo NICS računov, izračunov aktivacijskih energij in relativne stabilnosti (ΔE) posameznih struktur. Rezultati kažejo, da je mesto 1 v azulenu najbolj reaktivno za elektrofilne aromatske reakcije s kinetičnega vidika, medtem ko so izomerni produkti, substituirani na mestu 2, produkti termodinamsko kontrolirane reakcije.

Supplementary material



The structural data of intermediates (2) optimized at the B3LYP/6-31+G** level



The structural data of products (3) optimized at the B3LYP/6-31+G** level